ACOUSTICS 2012

On the use of periodic inclusions embedded in porous lining to enhanced attenuation in waveguides

B. Nennig[a], Y. Renou[b] and Y. Aurégan[b]

[a]Laboratoire d'Ingénierie des Systèmes Mécaniques et des MAtériaux, Supméca - 3, rue Fernand Hainaut - 93407 St Ouen Cedex
[b]Laboratoire d'acoustique de l'université du Maine, Bât. IAM - UFR Sciences Avenue Olivier Messiaen 72085 Le Mans Cedex 9
benoit.nennig@supmeca.fr

Acoustic liners are often used to limit noise propagation in acoustic waveguides with a grazing flow such as ventilation, exhaust or aircraft engine. Standard liners are most often made of perforated plate backed by honey comb or with porous material. The aim of this work is to study the influence of a set of periodic rigid inclusions embedded in a porous lining to enhanced attenuation. Only an elementary cell of this periodic waveguide is studied using the Bloch waves formalism. This yields a quadratic eigenvalue problem involving the Bloch wavenumber solved with the finite element method. However these configurations require to investigate parameters often omitted in academic lattice studies : (i) Dissipation; (ii) higher modes interaction; (iii) mean flow convection effect.
These absorbing concepts as well as the computational approach are validated with analytical solution on homogeneous waveguide. The influence of the inclusion shape, waveguide dimension and the mean flow impact are illustrated on various examples.

1 Introduction

Acoustic liners are often used to limit noise propagation in acoustic waveguides with a grazing flow such as ventilation systems, exhaust device or aircraft engine. In the latter case, these acoustic treatments are generally made with a perforated sheet backed by honeycomb [8]. This kind of material have good absorbing properties only in a narrow frequency band but their main advantages are their mechanical robustness and their capability to resist to harsh conditions i.e. they constitute the reference solution in a turbofan engine. For the other applications porous material are often used [20, 12, 17, 16] because they generally offer a wider absorption/attenuation band. See for instance the comparison presented in Ref. [2].

In the last decades in parallel to this well known concepts, very interesting results have been obtained in acoustics thanks to the presence of periodic geometrical discontinuity [4] or with periodic sequence of locally reacting material sequences [3, Chap. 5]. In such waveguide, the coherent effects of multiple reflection lead to frequency bands in which propagation of waves is forbidden, the so called band-gap. These works are in line with numerous studies on periodic structures in whole waves community e.g. optics [10] or in solid states physics. Always in acoustics, similar concepts have been used to enhance absorbing properties of porous material slab [7, 18] by embedding periodic inclusions. Thank to this approach, it is possible get total absorption peak below the quarter wave frequency or to widen the absorption in a specified range.

The aim of this paper, is to test the potentiality of periodic rigid inclusion embedded in a porous material for waveguide applications instead of acoustics gratings [7, 18]. However these configurations require to investigate parameters often omitted in academic lattice studies : (i) Dissipation [5]; (ii) higher modes interaction [22]; (iii) mean flow convection effect [15].

The dissipation is mostly neglected in the literature because band-gaps are the direct consequence of destructive interferences and can not occurred in too dissipative media. Although, porous material present strong dissipation and high dispersion, the attenuation in a waveguide results of a compromise between waveguide dimensions, the liner thickness and the porous material properties. In other words, interference is a good candidate to enhance the attenuation in the frequency range where the attenuation is too weak.

In order to investigate this kind of problem, it is assumed the waveguide is periodic and of infinite extent. The Floquet-Bloch theorem is used to reduce the computation on one period, leading to a quadratic eigenvalue problem. This assumption is not too strong since the infinite behavior is recovered when more than 4 or 6 cells are present [11]. To tackle this problem, a finite element (FE) method, inspired from Ref. [5], is chosen for its robustness and its ability to take into account complex geometries.

The present paper is organized as follows. After presenting the FE formulation in Section 2, a numerical example on U-shape inclusion are given.

2 Formulation of the method

2.1 Problem statement

We consider here the acoustic wave propagation in a 2D infinite periodic waveguide lined with a porous material with embedded rigid inclusions as described Fig. 1. In the acoustic domain Ω_a, ie $x_2 \in [0,\ h_a]$ the velocity potential $\hat{\phi}_a$ satisfy the convected wave equation

$$\Delta\hat{\phi}_a(\mathbf{x}) - \frac{1}{c_a^2}\frac{\mathrm{d}^2\hat{\phi}_a(\mathbf{x})}{\mathrm{d}t^2} = 0, \quad \forall \mathbf{x} \in \Omega_a, \tag{1}$$

where $\frac{\mathrm{d}}{\mathrm{d}t} \equiv (-\mathrm{i}\omega + U\partial_{x_1})$ stands for the material derivative along the mean flow with time-harmonic representation ($\mathrm{e}^{-\mathrm{i}\omega t}$ is omitted for clarity). For a brief nomenclature, t is time, c_a denotes the sound speed and U is the mean flow axial velocity and $M = U/c_a$ is the Mach number. It is convenient for the analysis to introduce the velocity potential to simplify the calculation. The acoustic velocity is simply $\hat{\mathbf{v}}_a = \nabla\hat{\phi}_a$ and pressure may be recovered by using $\hat{p}_a = -\rho_a\frac{\mathrm{d}\hat{\phi}_a}{\mathrm{d}t}$ where ρ_a is the fluid density.

In the porous material, ie $x_2 \in [-h_p,\ 0]$, the skeleton of the porous material is considered as infinitely rigid, thus the Champoux-Allard-Johnson equivalent fluid model [1] is used to get the equivalent bulk modulus $K_p(\omega)$ and density $\rho_p(\omega)$ (see Allard [1] for details). The celerity is given by the ratio $c_p(\omega) = \sqrt{K_p(\omega)/\rho_p(\omega)}$. Assuming there is no mean flow in the porous material, the velocity potential $\hat{\mathbf{v}}_p = \nabla\hat{\phi}_p$ satisfies the Helmholtz equation,

$$\Delta\hat{\phi}_p(\mathbf{x}) + k_p(\omega)^2\hat{\phi}_p(\mathbf{x}) = 0, \quad \forall \mathbf{x} \in \Omega_p, \tag{2}$$

with $k_p(\omega) = \omega/c_p(\omega)$. The pressure is then simply $\hat{p}_p = \mathrm{i}\omega\rho_p(\omega)\hat{\phi}_p$. Both media are coupled together at the interface Γ_c. Here we assume the continuity of the pressure and the continuity of the normal displacement hold[21], leading respectively to

$$\rho_p c_p \mathrm{i}k_p\hat{\phi}_p = -\rho_a c_a\left(-\mathrm{i}k_a + M\partial_{x_1}\right)\hat{\phi}_a, \tag{3a}$$

$$-\mathrm{i}\omega\partial_{n_a}\hat{\phi}_a = c_a\left(-\mathrm{i}k_a + M\partial_{x_1}\right)\partial_{n_a}\hat{\phi}_p, \tag{3b}$$

where $\mathbf{n}_i$ denotes the outward normal unit vector to ith domain with $i = a,\ p$. Note the continuity of the displacement

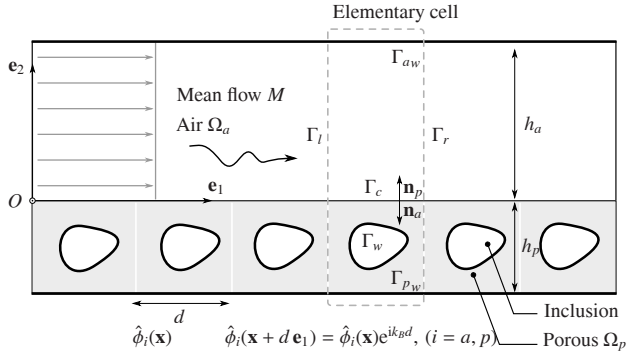

Figure 1: Geometry of the problem.

corresponds to the Ingard-Myers condition [9, 14] for parallel uniform mean flow. On the rigid walls Γ_{iw}, $(i = a, p)$, the normal velocity vanish and we get $\partial_{n_i}\hat{\phi}_i = 0$.

2.2 Bloch waves and eigenvalue problems

As the governing equation, the boundary condition and the geometry are d-periodic, it follows from the Floquet-Bloch theorem the solution are Bloch waves [10]

$$\hat{\phi}_i(\mathbf{x}) = \phi_i(\mathbf{x})\mathrm{e}^{\mathrm{i}k_B x_1}, \tag{4}$$

i.e. the velocity potential can be split into a d-periodic field $\phi_i(\mathbf{x})$ modulated by a plane wave with the Floquet Bloch wavenumber k_B. Note, the Bloch wavenumber is common for both media as the axial wavenumber for classical guided wave problems.

On the right and left boundary of the elementary cell, respectively on Γ_r and Γ_l, the velocity potential satisfies the condition

$$\hat{\phi}_i(\mathbf{x}+d\mathbf{e}_1) = \hat{\phi}_i(\mathbf{x})\mathrm{e}^{\mathrm{i}k_B d}, \text{ with } i = a,\ p. \tag{5}$$

It follows from (5) that the real part of k_B measures the change in phase across the cell and its imaginary part the attenuation. In addition, it can be directly shown from (4) that k_B is defined modulo $2\pi/d$. The smallest values belongs to the irreducible Brillouin zone.

By inserting (4) into (1), (2) and (3) we get respectively

$$\left(\Delta\phi_a - \frac{1}{c_a^2}\frac{\mathrm{d}^2\phi_a}{\mathrm{d}t^2}\right) + k_B\left(2\mathrm{i}\left(1-M^2\right)\partial_{x_1}\phi_a - 2kM\phi_a\right) - k_B^2(1-M^2)\phi_a = 0, \tag{6}$$

and

$$\left(\Delta\phi_p + k_p^2\phi_p\right) + 2\mathrm{i}k_B\partial_{x_1}\phi_p - k_B^2\phi_p = 0, \tag{7}$$

on both domain and

$$\rho_p c_p \mathrm{i}k_p\phi_p = -\rho_a c_a\left[-\mathrm{i}k_a + M\left(\partial_{x_1} + \mathrm{i}k_B\right)\right]\phi_a, \tag{8a}$$

$$-\mathrm{i}\omega\partial_n\phi_a = c_a\left[-\mathrm{i}k_a + M\left(\partial_{x_1} + \mathrm{i}k_B\right)\right]\partial_n\phi_p, \tag{8b}$$

on Γ_c. These equations (6)-(8) leads to an eigenvalue problem. The first terms in (6) and (7) correspond to the wave equation applied on the periodic fields ϕ_i $(i = a,\ p)$ and the others, involving k_B can be seen as the correction terms that force the periodic boundary condition. The resolution is generally performed by fixing k_B (real) and ω is considered as the eigenvalue. Propagating modes correspond to real frequency whereas evanescent modes (i.e. band gap) correspond to complex frequency. However, as in the porous media all coefficients are frequency dependent, the eigenvalue problem is highly non-linear in ω. Therefore, it is preferable to solve the quadratic eigenvalue problem at fixed ω values with k_B as eigenvalue[5]. This approach will be detailed in the next section.

2.3 Finite element discretisation

The associated weak formulation is obtained after multiplying (6) and (7) by a periodic test function $\bar{\psi}_i$, $(i = a,\ p)$, integrating over an elementary cell and ones integration by parts. This yields

$$\begin{aligned}\int_{\Omega_a}\left(-\nabla\bar{\psi}_a\cdot\nabla\phi_a + \frac{\bar{\mathrm{d}}\bar{\psi}_a}{\mathrm{d}t}\frac{\mathrm{d}\phi_a}{\mathrm{d}t}\right)\mathrm{d}\Omega \\ + k_B\int_{\Omega_a}\left(2\mathrm{i}(1-M^2)\bar{\psi}_a\partial_{x_1}\phi_a - 2k_aM\bar{\psi}_a\phi_a\right)\mathrm{d}\Omega, \\ - k_B^2(1-M^2)\int_{\Omega_a}\bar{\psi}_a\phi_a\,\mathrm{d}\Omega \\ - \int_{\partial\Omega_a}\left(\bar{\psi}_a M\mathbf{e}_1\cdot\mathbf{n}_a\frac{\mathrm{d}\phi_a}{\mathrm{d}t} - \bar{\psi}_a\frac{\partial\phi_a}{\partial n_a}\right)\mathrm{d}\Gamma = 0.\end{aligned} \tag{9}$$

for the convected Helmholtz equation with $\frac{\bar{\mathrm{d}}}{\mathrm{d}t} \equiv (\mathrm{i}\omega + U\partial_{x_1})$. The weak formulation in the porous media is deduced by putting $M = 0$ and switching the subscript a and p. The global formulation is obtained by summing the weak formulation of both domain Ω_a and Ω_p.

The last step is to impose the boundary conditions on $\partial\Omega_i = \Gamma_c \cup \Gamma_{ir} \cup \Gamma_{il} \cup \Gamma_{iw}$. On the rigid wall Γ_{i_r}, the condition $\partial_{n_i}\hat{\phi}_i = 0$ leads to

$$\partial_{n_i}\phi_i = -\mathrm{i}k_B(\mathbf{e}_1\cdot\mathbf{n}_i)\phi_i. \tag{10}$$

On the waveguide wall, the standard Neumann condition is recovered since $\mathbf{e}_1\cdot\mathbf{n}_i = 0$. However, on inclusion walls, the correction term must be taken into account.

On the lateral boundary, due to the periodicity condition on ϕ, the boundary integrals vanish. Note the degree of freedom related to the Γ_{ir} are re-expressed with respect to those of Γ_{il} and the problem is finally solved with a reduced set of unknown, as done in Ref. [19] (excepted we are solving directly the periodic field).

Let us focus now on the Γ boundary. As the mean flow is parallel to the duct, the first term of the boundary integral vanishes. It remains

$$+\int_{\Gamma_c}\bar{\psi}_a\frac{\partial\phi_a}{\partial n_a}\,\mathrm{d}\Gamma + \int_{\Gamma_c}\bar{\psi}_p\frac{\partial\phi_p}{\partial n_p}\,\mathrm{d}\Gamma. \tag{11}$$

However imposing coupling condition is a little more tricky and require Lagrange multiplier. We introduce $\lambda = \partial_{n_a}\phi_p$ and its associated test function $\bar{\lambda'}$. Using (8b) in the previsous expression yields the two first integrals in

$$\begin{aligned}\frac{c_a}{-\mathrm{i}\omega}\int_{\Gamma_c}\bar{\psi}_a\left[\left(-\mathrm{i}k_a + M\partial_{x_1}\right)\lambda + \mathrm{i}k_BM\lambda\right]\mathrm{d}S \\ - \int_{\Gamma_c}\bar{\psi}_p\lambda\,\mathrm{d}S + \frac{1}{-\mathrm{i}\omega}\int_{\Gamma_c}\bar{\lambda'}\left[\rho_a c_a\left(-\mathrm{i}k_a + M\partial_{x_1}\right)\phi_a \right. \\ \left. +\rho_a c_a M\mathrm{i}k_B\phi_a + \mathrm{i}\omega\rho_p\phi_p\right]\mathrm{d}S,\end{aligned} \tag{12}$$

and the pressure continuity (8a) is weakly added thanks to $\overline{\lambda}'$ in the last integral.

Once the power of k_B have been collected, we get the following quadratic eigenvalue problem in k_B

$$K_0 + K_1 k_B + K_2 k_B^2 = 0, \tag{13}$$

where K_i ($i = 0, \ldots, 2$) are combination of bilinear operator involving the test function, the periodic potential and the Lagrange multiplier. The discretisation of K_i operators are carried out using Lagrange quadratic finite elements in both fluid and porous domains, excepted for the Lagrange multiplier for which a linear discretization is required to avoid spurious modes. The mesh were performed with Gmsh [6]. The FE implementation (integration, matrix assembly and eigenvalue problem) is carried out on Matlab. The first twenty eigenvalues of smallest magnitudes are solved with implicitly restarted Arnoldi method [13] once the quadratic eigenvalue problem has be recasted into an equivalent generalized eigenvalue problem of double the dimension.

The convergence of the method has been investigated on homogeneous waveguide with an arbitrary period d. It has be shown the error decreases as h^4, where h is the element length. In this case, a relative error of 1% can be achieved with 10 quadratic elements per period for the first four modes.

3 Results on U-shape inclusions

In this section, we are interested in U-shape inclusions (see Fig. 2) embedded in a metal foam (see Tab. 1). These scatterers are located at the center of the periodic cell with the dimensions : $h_a = 135$ mm, $h_p = 20$ mm and $d = 15$ mm. The modal attenuation in dB/m, given by

$$A(k_B) = 8.68 \cdot \Im\mathrm{m} k_B, \tag{14}$$

can be shown for such configuration in Fig. 3. A significant enhancement can be observed compare to the homogeneous porous liner (in blue) over the whole bandwidth. In addition, the first attenuation peak amplitude is twice higher and a second peak emerges around 5000 Hz.

To explain this behavior, the band diagram, obtained by plotting the Bloch wave number according to the frequency, is presented in Fig. 2. The band diagram summarizes all dispersion properties of the waveguide. When $k_B < 0.5$ and the frequency is not too high, the periodic wave guide can interpreted in the homogeneous waveguide framework. For example it can be observed the phase velocity of most of the modes tend to c_0 excepted for the first cut-off mode. In this case, the phase velocity limit is lower than the celerity in the homogeneous porous material and is related to the presence of the inclusions. This phenomenon can be used to defined a new tortuosity at the mesoscopic scale. After the crossing with the fundamental mode towards 1700 Hz, this mode remains localized in the liner and a good approximation can be obtained by solving the Bloch eigenvalue problem in the liner alone, assuming $p_p = 0$ boundary condition on the coupling interface Γ_c (see $*$ marker in Fig. 2). It is worth noting that the first attenuation peak is strongly connected to this crossing. Indeed, modes avoid each other thank to a modification of the k_B imaginary part leading to an enhancement of the attenuation. Similar explications may hold for the second peak. In this case, the fundamental and the second cut-off

Table 1: Materials properties used in numerical tests. With the porosity ϖ, flow resistivity σ, the tortuosity α_{inf}, the viscous and thermal characteristic lengths Λ and Λ'.

Material	ϖ	σ	α_{inf}	Λ	Λ'	Ref.
	-	[kNm^{-4}s]	-	[μm]	[μm]	
Metal foam	0.99	6.916	1.17	100	245	-

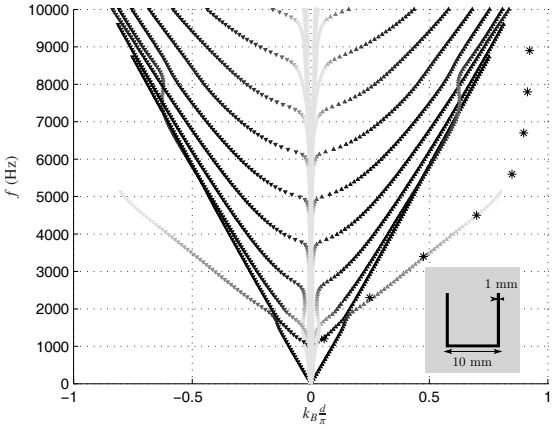

Figure 2: Band diagram for U-shape inclusions. The gray scale indicates the magnitude of the imaginary part of k_B. The darkest are the line the smallest is the imaginary part. The sign of the imaginary part is given by the markers orientation, '+' is denoted by ▲ and '−' is denoted by ▼. The marker ($*$) indicates the dispersion curves for the first mode of the liner alone with $p = 0$ condition on Γ_c interface.

modes Bloch wave number are very closed and a shift in the imaginary part of k_B is also observed.

Now, when $k_B > 0.5$, the lattice effects becomes visible. Around 5 kHz, a band gap reminiscence appears. Band band gap cannot be present in lossy media but the right and left traveling waves strongly interact between 5 and 10 kHz and increase drastically the attenuation of the mode localized in the liner. Another noticeable behavior associated with negative group velocity can also be noted between 7.5 and 8 kHz. This phenomenon seem to be linked with higher order mode quasi band gap.

.

4 Conclusions and prospects

This work investigates the presence of rigid scatterers embedded in a porous material liner. It has been shown that open shape inclusions (e.g. U-shape) are able to enhance the attenuation when compared with a homogeneous liner. Moreover, rigid inclusions combined with metal foam is an interesting way to achieve a compact, efficient acoustic treatment for a harsh environment or when good structural behavior is required. Future works can focus on exploring new inclusion shapes and to develop some simplified models through homogenization procedure.

Acknowledgment

The authors acknowledge the FUI project REBECCA and their industrial partners in this project: Snecma and SPS.

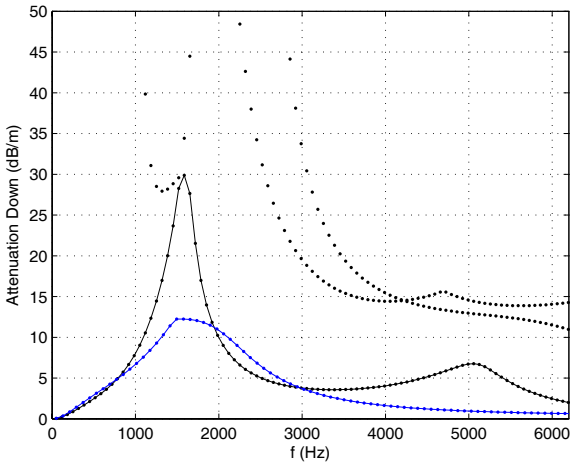

Figure 3: Attenuation of the first the heterogeneous liner modes (black) compared with the first homogeneous porous material mode (blue).

References

[1] J.-F. Allard. *Propagation of Sound in Porous Media: Modeling Sound Absorbing Materials*, page 280pp. Chapman & Hall, 1993.

[2] R. J. Astley. A comparative note on the effects of local versus bulk reaction models for air moving ducts lined on all sides. *J. Sound Vib.*, 117(1):191–197, 1987.

[3] W. Bi. *Propagation acoustique dans les guides a section variable traités aux parois par impédance nonuniforme (Sound propagation in varying cross-section waveguides with non-uniform boundary conditions)*. PhD thesis, Université du Maine, France, 2004.

[4] C. E. Bradley. Time harmonic acoustic Bloch wave propagation in periodic waveguides. part i. theory. *J. Acoust. Soc. Am.*, 96(3):1844–1853, 1994.

[5] C. Engström, C. Hafner, and K. Schmidt. Computations of lossy Bloch waves in two-dimensional photonic crystals. *J. Comput. Theor. Nanosci.*, 6:775–783, 2009.

[6] C. Geuzaine and J.-F. Remacle. Gmsh: a three-dimensional finite element mesh generator with built-in pre- and post-processing facilities. *Int. J. Num. Meth. Eng.*, 79(11):1309–1331, 2009.

[7] J.-P. Groby, A. Duclos, O. Dazel, L. Boeckx, and W. Lauriks. Enhancing absorption coefficient of a backed rigid frame porous layer by embedding circular periodic inclusions. *J. Acoust. Soc. Am.*, 130(5):3071–3780, 2011.

[8] H. H. Hubbard. *Aeroacoustics of Flight Vehicles: Theory and Practice*. 1995.

[9] K. U. Ingard. Influence of fluid motion past a plane boundary on sound reflection, absorption and transmission. *J. Acoust. Soc. Am.*, 31(7), 1959.

[10] J. D. Joannopoulos, R. D. Meade, and J. N. Winn. *Photonic Crystals: Molding the Flow of Light, 2nd ed.*, page 286pp. Princeton University Press, New Jersey, 2008.

[11] P. D. C. King and T. J. Cox. Acoustic band gaps in periodically and quasiperiodically modulated waveguides. *J. Appl. Phy.*, 102:014902–1–014902–8, 2007.

[12] J. B. Lawrie and R. Kirby. Mode-matching without root-finding: Application to a dissipative silencer. *J. Acoust. Soc. Am.*, 119(4):2050–2061, 2006.

[13] R.B. Lehoucq, D.C. Sorensen, and C. Yang. *ARPACK Users Guide: Solution of Large-Scale Eigenvalue Problems with Implicitly Restarted Arnoldi Methods*, page 140pp. SIAM Publications, Philadelphia, 1998.

[14] M. K. Myers. On the acoustic boundary condition in the presence of flow. *J. Sound Vib.*, 71(3):429–434, 1980.

[15] A. H. Nayfeh. Acoustic waves in ducts with sinusoidally perturbed walls and mean flow. *J. Acoust. Soc. Am.*, 957(5):1036–1039, 1975.

[16] B. Nennig, M. Ben Tahar, and E. Perrey-Debain. A displacement-pressure finite element formulation for analyzing the sound transmission in ducted shear flows with finite poroelastic lining. *J. Acoust. Soc. Am.*, 130(1):42–51, 2011.

[17] B. Nennig, E. Perrey-Debain, and M. Ben Tahar. A mode matching method for modelling dissipative silencers lined with poroelastic materials and containing mean flow. *J. Acoust. Soc. Am.*, 128(6):3308–3320, 2010.

[18] B. Nennig, Y. Renou, J.-P. Groby, and Y. Aurégan. A mode matching approach for modeling two dimensional porous grating with infinitely rigid or soft inclusions. *J. Acoust. Soc. Am.*, (In Press), 2012.

[19] A. Nicolet, S. Guenneau, C. Geuzaine, and F. Zolla. Modelling of electromagnetic waves in periodic media with finite elements. *J. Comput. Appl. Math.*, 168:321 – 329, 2004.

[20] B. Nilsson and O. Brander. The propagation of sound in cylindrical ducts with mean flow and bulk-reacting lining. I. modes in an infinite duct. *J. Inst. Maths. Applics.*, 26:269–298, 1980.

[21] Y. Renou and Y. Aurégan. Failure of the Ingard–Myers boundary condition for a lined duct: An experimental investigation. *J. Acoust. Soc. Am.*, 130(1):52–69, 2011.

[22] Z. Tao, W.-Y. He, and X. Wang. Sound transmission within the Bragg gap via the high-order modes in a waveguide with periodically corrugated walls. *J. Appl. Phys.*, 105(12):123515–123522, 2009.